International Journal of Physics, 2017, Vol. 5, No. 1, 9-15
Available online at http://pubs.sciepub.com/ijp/5/1/2

DOI:10.12691/ijp-5-1-2

Structural-Parametric Model Electromagnetoelastic Actuator Nanodisplacement for Mechatronics

Sergey Mikhailovich Afonin*

Department of Intellectual Technical Systems, National Research University of Electronic Technology (MIET), Moscow, Russia
*Corresponding author: eduems@mail.ru

Abstract Electromagnetoelastic actuator have been used successfully to nanodisplacement for mechatronics systems in nanotechnology, electronic engineering, microelectronics, nanobiology, power engineering, astronomy. Linear structural-parametric model, parametric structural schematic diagram, transfer functions of the simple electromagnetoelastic actuator nanodisplacement for the mechatronics systems are obtained. For calculation of the mechatronics system with piezoactuator the parametric structural schematic diagram and the transfer functions of the piezoactuator are obtained. A generalized parametric structural schematic diagram and transfer functions of the piezoactuator are constructed. This work describes the linear structural-parametric model of the simple piezoactuator for the mechatronic in the static and dynamic operation modes in contrast solving its electrical equivalent circuit.

Keywords: *electromagnetoelastic actuators, structural-parametric model, piezoactuator, deformation, nanodisplacement, transfer functions*

Cite This Article: Sergey Mikhailovich Afonin, "Structural-Parametric Model Electromagnetoelastic Actuator Nanodisplacement for Mechatronics." *International Journal of Physics*, vol. 5, no. 1 (2017): 9-15. doi: 10.12691/ijp-5-1-2.

1. Introduction

For mechatronics, nanotechnology, electronic engineering, microelectronics, nanobiology, power engineering, astronomy, antennas satellite telescopes and adaptive optics are promising the electromechanical actuators based on electromagnetoelasticity (piezoelectric, piezomagnetic, electrostriction, and magnetostriction effects). Piezoactuator - piezomechanical device intended for actuation of mechanisms, systems or management based on the piezoelectric effect, converts electrical signals into mechanical movement or force. Piezoactuators are used in the majority of scanning tunneling microscopes (STMs), atomic force microscopes (AFMs), in the adaptive optics of big telescopes, for example, European Extremely Large Telescope (E-ELT) and Large Synoptic Survey Telescope (LSST) [1-25].

In the present paper is solving the problem of building the linear structural-parametric model of the simple electromagnetoelastic actuator nanodisplacement the mechatronics systems for static and dynamic operation modes in contrast solving its electrical equivalent circuit Cady-Mason. Equivalent circuits of the piezoelectric transducers are designed for calculation of piezoelectric transmitters and receivers [9,10,11,12]. For the next new paper about the control system of the piezoactuator will be used, for example, the nonlinear hysteresis model for correction control system of the piezoactuator [8].

By solving the wave equation with allowance methods of mathematical physics for equation electromagnetoelasticity, the boundary conditions on loaded working surfaces of actuators, the strains along the coordinate axes, it is possible to construct the linear structural-parametric model of the actuator for the mechatronics systems [14-23].

2. The Structural-Parametric Model of the Electromagnetoelastic Actuator for Mechatronics Systems

For the piezoactuator its deformation corresponds to stressed state. If the mechanical stress T is created in the piezoelectric element, the deformation S is formed in it.

There are six stress components T_1, T_2, T_3, T_4, T_5, T_6, the components T_1 - T_3 are related to extension-compression stresses, T_4 - T_6 to shear stresses.

The matrix state equations [12] connecting the electric and elastic variables for polarized ceramics for the mechatronics systems have the form

$$\mathbf{D} = \mathbf{dT} + \boldsymbol{\varepsilon}^T \mathbf{E}, \quad (1)$$

$$\mathbf{S} = \mathbf{s}^E \mathbf{T} + \mathbf{d}^t \mathbf{E}, \quad (2)$$

where the first equation describes the direct piezoelectric effect, and the second - the inverse piezoelectric effect; $\mathbf{D}$ is the column matrix of electric induction along the coordinate axes; $\mathbf{S}$ is the column matrix of relative deformations; $\mathbf{T}$ is the column matrix of mechanical stresses; $\mathbf{E}$ is the column matrix of electric field strength along the coordinate axes; $\mathbf{s}^E$ is the elastic compliance matrix for $E = \text{const}$; $\boldsymbol{\varepsilon}^T$ is the matrix of the dielectric

permeabilities for $T = \text{const}$; $\mathbf{d}^t$ is the transposed matrix of the piezoelectric modules. In polarized ceramics PZT there are five independent components s_{11}^E, s_{12}^E, s_{13}^E, s_{33}^E, s_{55}^E in the elastic compliance matrix for polarized piezoelectric ceramics, three independent components of the piezoelectric modules d_{33}, d_{31}, d_{15} in the transposed matrix of the piezoelectric modules and three independent components of the dielectric constants $\varepsilon_{11}^{\mathrm{T}}$, $\varepsilon_{22}^{\mathrm{T}}$, $\varepsilon_{33}^{\mathrm{T}}$ in the matrix of dielectric constants.

The direction of the polarization axis P, i.e., the direction along which polarization was performed, is usually taken as the direction of axis 3.

The generalized electromagnetoelasticity equation of the actuator [12] for mechatronics systems has the form

$$S_i = s_{ij}^{E,H,\Theta} T_j + d_{mi}^{H,\Theta} E_m + d_{mi}^{E,\Theta} H_m + \alpha_i^{E,H} \Delta\Theta, \quad (3)$$

where S_i is the relative deformation along the axis i, E is the electric field strength, H is the magnetic field strength, Θ is the temperature, $s_{ij}^{E,H,\Theta}$ is the elastic compliance for $E = \text{const}$, $H = \text{const}$, $\Theta = \text{const}$, T_j is the mechanical stress along the axis j, $d_{mi}^{H,\Theta}$ is the piezomodule, i.e., the partial derivative of the relative deformation with respect to the electric field strength for constant magnetic field strength and temperature, i.e., for $H = \text{const}$, $\Theta = \text{const}$, E_m is the electric field strength along the axis m, $d_{mi}^{E,\Theta}$ is the magnetostriction coefficient, H_m is the magnetic field strength along the axis m, $\alpha_i^{E,H}$ is the coefficient of thermal expansion, $\Delta\Theta$ is deviation of the temperature Θ from the value $\Theta = \text{const}$, i = 1, 2, … , 6, j = 1, 2, … , 6, m = 1, 2, 3.

Let us consider the simplest electromagnetoelastic actuators for longitudinal, transverse and shift deformations in contrast the bimorph flextensional piezoactuators [1,2,3]. Piezoactuator for the longitudinal piezoelectric effect are shown in Figure 1, where δ is the thickness. The electrodes deposited on its faces perpendicular to axis 3, the area of face is equal to S_0. In the equation (2) of the inverse longitudinal piezoelectric effect are the following parameters: $S_3 = \partial\xi(x,t)/\partial x$ is the relative displacement of the cross section of the piezoactuator, d_{33} is the piezomodule for the longitudinal piezoelectric effect, $E_3(t) = U(t)/\delta$ is the electric field strength, $U(t)$ is the voltage between the electrodes of actuator, δ is the thickness, s_{33}^E is the elastic compliance along axis 3, and T_3 is the mechanical stress along axis 3.

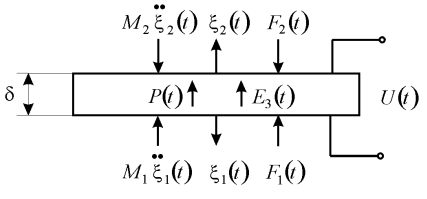

Figure 1. Piezoactuator for the longitudinal piezoelectric effect

Simultaneously solved the wave equation, the equation of the inverse longitudinal piezoeffect and the equation of forces acting on the faces of the piezoactuator. Calculations of the piezoactuators are performed using a wave equation [2,12] describing a wave propagation in a long line with damping but without distortions, in the form

$$\frac{1}{(c^E)^2}\frac{\partial^2\xi(x,t)}{\partial t^2} + \frac{2\alpha}{c^E}\frac{\partial\xi(x,t)}{\partial t} + \alpha^2\xi(x,t) = \frac{\partial^2\xi(x,t)}{\partial x^2}, \quad (4)$$

where $\xi(x,t)$ is the displacement of the section, x is the coordinate, t is time, c^E is the sound speed for $E = \text{const}$, α is the damping coefficient.

Using the Laplace transform, we can reduce the original problem for the partial differential hyperbolic equation of type (4) to a simpler problem for the linear ordinary differential equation [2,3,13,14].

Applying the Laplace transform to the wave equation (4) and setting the zero initial conditions, we obtain the linear ordinary second-order differential equation with the parameter p

$$\frac{d^2\Xi(x,p)}{dx^2} - \left[\frac{1}{(c^E)^2}p^2 + \frac{2\alpha}{c^E}p + \alpha^2\right]\Xi(x,p) = 0. \quad (5)$$

Solution of the linear ordinary second-order differential equation is the function

$$\Xi(x,p) = Ce^{-x\gamma} + Be^{x\gamma}, \quad (6)$$

where $\Xi(x,p)$ is the Laplace transform of the displacement of the section of the actuator, $\gamma = p/c^E + \alpha$ is the propagation coefficient. Coefficients C and B of the solution of the linear ordinary second-order differential equation are determined for the conditions

$$\begin{aligned} &\Xi(0,p) = \Xi_1(p) \text{ for } x = 0, \\ &\Xi(\delta,p) = \Xi_2(p) \text{ for } x = \delta. \end{aligned} \quad (7)$$

Then, the coefficients are the following form:

$$\begin{aligned} C &= \left(\Xi_1 e^{\delta\gamma} - \Xi_2\right)\Big/\left[2\mathrm{sh}(\delta\gamma)\right], \\ B &= -\left(\Xi_1 e^{-\delta\gamma} - \Xi_2\right)\Big/\left[2\mathrm{sh}(\delta\gamma)\right]. \end{aligned} \quad (8)$$

The solution (5) can be written as

$$\Xi(x,p) = \left\{\begin{matrix}\Xi_1(p)\mathrm{sh}\left[(\delta - x)\gamma\right] \\ +\Xi_2(p)\mathrm{sh}(x\gamma)\end{matrix}\right\}\Big/\mathrm{sh}(\delta\gamma). \quad (9)$$

The equations for the forces on the faces of the piezoactuator

$$\begin{aligned} &T_3(0,p)S_0 = F_1(p) + M_1 p^2\Xi_1(p) \text{ for } x = 0, \\ &T_3(\delta,p)S_0 = -F_2(p) + M_2 p^2\Xi_1(p) \text{ for } x = \delta, \end{aligned} \quad (10)$$

where $T_3(0,p)$ and $T_3(\delta,p)$ are determined from the equation of the inverse piezoelectric effect.

For $x = 0$ and $x = \delta$, we obtain the following set of the equations for determining stresses in the piezoactuator [15-24]

$$T_3(0,p)=\frac{1}{s_{33}^E}\frac{d\Xi(x,p)}{dx}\Big|_{x=0}-\frac{d_{33}}{s_{33}^E}E_3(p),$$
$$T_3(\delta,p)=\frac{1}{s_{33}^E}\frac{d\Xi(x,p)}{dx}\Big|_{x=\delta}-\frac{d_{33}}{s_{33}^E}E_3(p). \quad (11)$$

The set of equations (5) yield the set of equations for the linear structural-parametric model of the piezoactuator and parametric structural schematic diagram of a voltage-controlled piezoactuator for longitudinal piezoelectric effect Figure 2:

$$\Xi_1(p)=\left[1/\left(M_1p^2\right)\right]\cdot$$
$$\left\{-F_1(p)+\left(1/\chi_{33}^E\right)\begin{bmatrix}d_{33}E_3(p)\\-\left[\gamma/\mathrm{sh}(\delta\gamma)\right]\begin{bmatrix}\mathrm{ch}(\delta\gamma)\Xi_1(p)\\-\Xi_2(p)\end{bmatrix}\end{bmatrix}\right\}, \quad (12)$$

$$\Xi_2(p)=\left[1/\left(M_2p^2\right)\right]\cdot$$
$$\left\{-F_2(p)+\left(1/\chi_{33}^E\right)\begin{bmatrix}d_{33}E_3(p)\\-\left[\gamma/\mathrm{sh}(\delta\gamma)\right]\begin{bmatrix}\mathrm{ch}(\delta\gamma)\Xi_2(p)\\-\Xi_1(p)\end{bmatrix}\end{bmatrix}\right\},$$

where $\chi_{33}^E=s_{33}^E/S_0$.

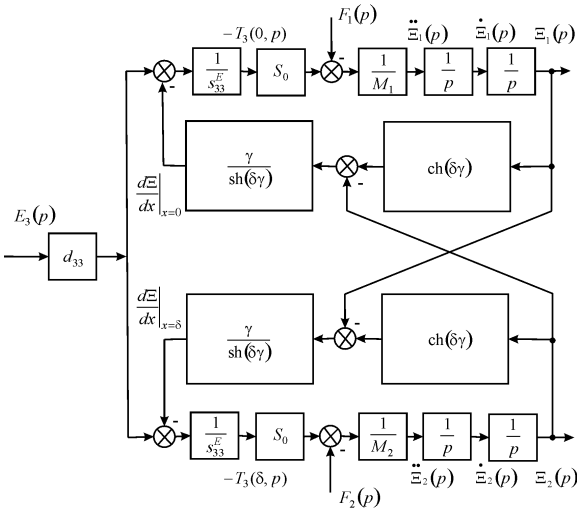

Figure 2. Parametric structural schematic diagram of a voltage-controlled piezoactuator for longitudinal piezoelectric effect

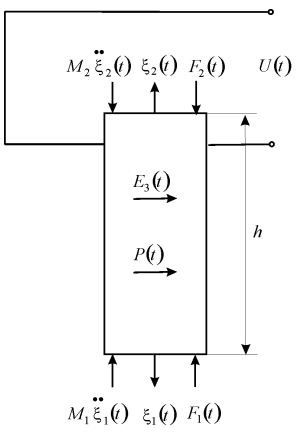

Figure 3. Piezoactuator for the transverse piezoelectric effect

In the equation (2) of the inverse transverse piezoeffect [12,14,15] are the following parameters: $S_1=\partial\xi(x,t)/\partial x$ is the relative displacement of the cross section along axis 1 Figure 3, d_{31} is the piezomodule for the transverse piezoeffect, s_{11}^E is the elastic compliance along axis 1, T_1 is the stress along axis 1.

The solution of the linear ordinary differential equation (5) can be written as (6), where the constants C and B in the form

$$\Xi(0,p)=\Xi_1(p) \text{ for } x=0,$$
$$\Xi(l,p)=\Xi_2(p) \text{ for } x=h, \quad (13)$$

$$C=\left(\Xi_1e^{h\gamma}-\Xi_2\right)/\left[2\mathrm{sh}(h\gamma)\right],$$
$$B=-\left(\Xi_1e^{-h\gamma}-\Xi_2\right)/\left[2\mathrm{sh}(h\gamma)\right]. \quad (14)$$

Then, the solution (5) can be written as

$$\Xi(x,p)=\begin{Bmatrix}\Xi_1(p)\mathrm{sh}\left[(h-x)\gamma\right]\\+\Xi_2(p)\mathrm{sh}(x\gamma)\end{Bmatrix}\Big/\mathrm{sh}(h\gamma). \quad (15)$$

The equations of forces acting on the faces of the piezoactuator

$$T_1(0,p)S_0=F_1(p)+M_1p^2\Xi_1(p) \text{ for } x=0, \quad (16)$$
$$T_1(h,p)S_0=-F_2(p)+M_2p^2\Xi_2(p) \text{ for } x=h,$$

where

$$T_1(0,p)=\frac{1}{s_{11}^E}\frac{d\Xi(x,p)}{dx}\Big|_{x=0}-\frac{d_{31}}{s_{11}^E}E_3(p), \quad (17)$$
$$T_1(h,p)=\frac{1}{s_{11}^E}\frac{d\Xi(x,p)}{dx}\Big|_{x=h}-\frac{d_{31}}{s_{11}^E}E_3(p).$$

The set of equations describing the linear structural-parametric model and parametric structural schematic diagram and parametric structural schematic diagram of a voltage-controlled piezoactuator for transverse piezoelectric effect Figure 4

$$\Xi_1(p)=\left[1/\left(M_1p^2\right)\right]\cdot$$
$$\left\{-F_1(p)+\left(1/\chi_{11}^E\right)\begin{bmatrix}d_{31}E_3(p)\\-\left[\gamma/\mathrm{sh}(h\gamma)\right]\begin{bmatrix}\mathrm{ch}(h\gamma)\Xi_1(p)\\-\Xi_1(p)\end{bmatrix}\end{bmatrix}\right\}, \quad (18)$$

$$\Xi_2(p)=\left[1/\left(M_2p^2\right)\right]\cdot$$
$$\left\{-F_2(p)+\left(1/\chi_{11}^E\right)\begin{bmatrix}d_{31}E_3(p)\\-\left[\gamma/\mathrm{sh}(h\gamma)\right]\begin{bmatrix}\mathrm{ch}(h\gamma)\Xi_2(p)\\-\Xi_1(p)\end{bmatrix}\end{bmatrix}\right\},$$

where $\chi_{11}^E=s_{11}^E/S_0$.

Let us consider the piezoactuator for the shift piezoelectric effect (2) on Figure 5.

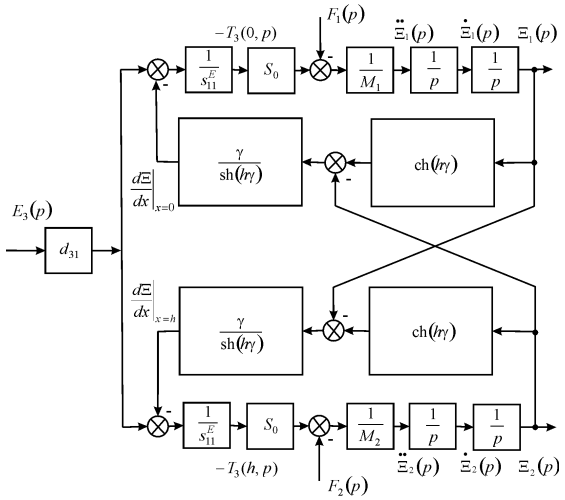

Figure 4. Parametric structural schematic diagram of a voltage-controlled piezoactuator for transverse piezoelectric effect

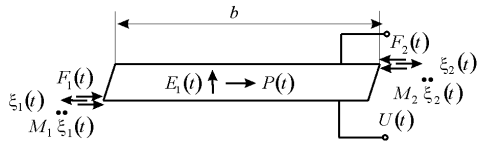

Figure 5. Piezoactuator for the shift piezoelectric effect

We obtain the following set of equations describing the structural-parametric model and schematic diagram Fig. 6

$$\Xi_1(p)=\left[1/\left(M_1p^2\right)\right]\cdot$$

$$\left\{-F_1(p)+\left(1/\chi_{55}^{E}\right)\begin{bmatrix}d_{15}E_1(p)\\-\left[\gamma/\mathrm{sh}\left(b\gamma\right)\right]\begin{bmatrix}\mathrm{ch}\left(b\gamma\right)\Xi_1(p)\\-\Xi_1(p)\end{bmatrix}\end{bmatrix}\right\},\quad(19)$$

$$\Xi_2(p)=\left[1/\left(M_2p^2\right)\right]\cdot$$

$$\left\{-F_2(p)+\left(1/\chi_{55}^{E}\right)\begin{bmatrix}d_{15}E_1(p)\\-\left[\gamma/\mathrm{sh}\left(b\gamma\right)\right]\begin{bmatrix}\mathrm{ch}\left(b\gamma\right)\Xi_2(p)\\-\Xi_1(p)\end{bmatrix}\end{bmatrix}\right\},$$

where $\chi_{55}^{E}=s_{55}^{E}/S_0$.

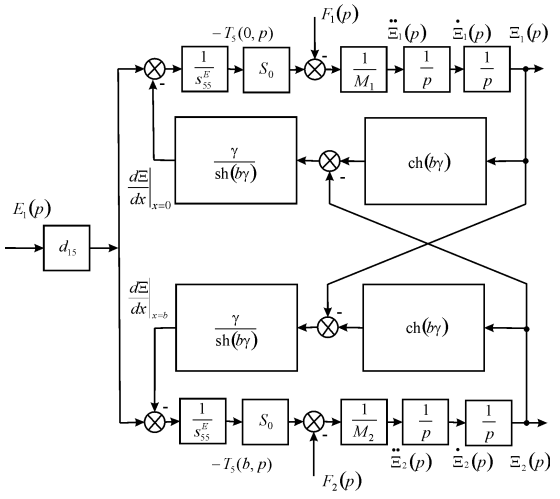

Figure 6. Parametric structural schematic diagram of a voltage-controlled piezoactuator for shift piezoelectric effect

From (2), (3), (12), (18), (19) we obtain the system of equations describing the generalized linear structural-parametric model of the electromagnetoelastic actuator for the mechatronics systems

$$\Xi_1(p)=\left[1/\left(M_1p^2\right)\right]\cdot$$

$$\left\{-F_1(p)+\left(1/\chi_{ij}^{\Psi}\right)\begin{bmatrix}\nu_{mi}\Psi_m(p)\\-\left[\gamma/\mathrm{sh}\left(l\gamma\right)\right]\begin{bmatrix}\mathrm{ch}\left(l\gamma\right)\Xi_1(p)\\-\Xi_2(p)\end{bmatrix}\end{bmatrix}\right\},\quad(20)$$

$$\Xi_2(p)=\left[1/\left(M_2p^2\right)\right]\cdot$$

$$\left\{-F_2(p)+\left(1/\chi_{ij}^{\Psi}\right)\begin{bmatrix}\nu_{mi}\Psi_m(p)\\-\left[\gamma/\mathrm{sh}\left(l\gamma\right)\right]\begin{bmatrix}\mathrm{ch}\left(l\gamma\right)\Xi_2(p)\\-\Xi_1(p)\end{bmatrix}\end{bmatrix}\right\},$$

$$\chi_{ij}^{\Psi}=s_{ij}^{\Psi}/S_0,\nu_{mi}=\begin{cases}d_{33},d_{31},d_{15}\\g_{33},g_{31},g_{15},\Psi_m=\begin{cases}E_3,E_1\\D_3,D_1,\\H_3,H_1\end{cases}\\d_{33},d_{31},d_{15}\end{cases}$$

$$s_{ij}^{\Psi}=\begin{cases}s_{33}^{E},s_{11}^{E},s_{55}^{E}\\s_{33}^{D},s_{11}^{D},s_{55}^{D},c^{\Psi}=\begin{cases}c^{E}\\c^{D},\gamma=\begin{cases}\gamma^{E}\\\gamma^{D},l=\begin{cases}\delta\\h,\\b\end{cases}\end{cases}\end{cases}\\s_{33}^{H},s_{11}^{H},s_{55}^{H}\end{cases}$$

where the parameter Ψ of the control parameter for the electromagnetoelastic actuator: E for voltage control, D for current control, H for magnetic field strength control; s_{ij}^{Ψ} - elastic compliance at $\Psi=\mathrm{const}$; d_{33},d_{31},d_{15} - piezomodules; g_{33},g_{31},g_{15} - piezoelectric constants; c^{Ψ} - speed of sound at $\Psi=\mathrm{const}$; l - geometrical size in the deformation direction accordingly equal to δ, h, b - thickness, height or width of the electromagnetoelastic actuator; S_0 - area of the corresponding cross-section of the actuator.

On Figure 7 shows the generalized parametric structural schematic diagram of the electromagnetoelastic actuator corresponding to the set of equations (20) of the actuator for the mechatronics systems.

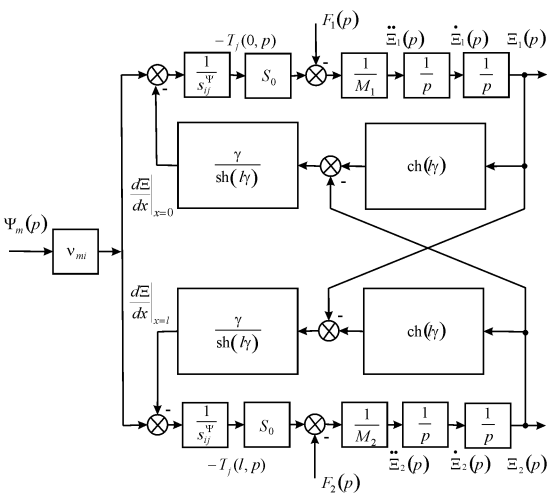

Figure 7. Generalized parametric structural schematic diagram of the electromagnetoelastic actuator

3. Transfer Functions of Electromagnetoelastic Actuator for Mechatronics Systems

We consider the construction of the transfer functions from the generalized structural-parametric model (20) of the electromagnetoelastic actuator for mechatronics systems.

After algebraic transformations of the generalized structural-parametric model of the actuator we provided the transfer functions of the actuator in matrix form [14-23], where the transfer functions are the ratio of the Laplace transforms of the displacement of the face actuator and the corresponding parameter or force at zero initial conditions.

$$\Xi_1(p) = W_{11}(p)\Psi_m(p) + W_{12}(p)F_1(p) + W_{13}(p)F_2(p), \quad (21)$$

$$\Xi_2(p) = W_{21}(p)\Psi_m(p) + W_{22}(p)F_1(p) + W_{23}(p)F_2(p),$$

where the generalized transfer functions of the electromagnetoelastic actuator are the following form:

$$W_{11}(p) = \Xi_1(p)/\Psi_m(p) = \nu_{mi}\left[M_2\chi_{ij}^{\Psi}p^2 + \gamma\,\mathrm{th}(l\gamma/2)\right]/A_{ij}, \quad (22)$$

$$A_{ij} = M_1M_2\left(\chi_{ij}^{\Psi}\right)^2 p^4 + \left\{(M_1+M_2)\chi_{ij}^{\Psi}/\left[c^{\Psi}\,\mathrm{th}(l\gamma)\right]\right\}p^3 + \left[(M_1+M_2)\chi_{ij}^{\Psi}\alpha/\mathrm{th}(l\gamma) + 1/\left(c^{\Psi}\right)^2\right]p^2 + 2\alpha p/c^{\Psi} + \alpha^2,$$

$$W_{21}(p) = \Xi_2(p)/\Psi_m(p) = \nu_{mi}\left[M_1\chi_{ij}^{\Psi}p^2 + \gamma\,\mathrm{th}(l\gamma/2)\right]/A_{ij}, \quad (23)$$

$$W_{12}(p) = \Xi_1(p)/F_1(p) = -\chi_{ij}^{\Psi}\left[M_2\chi_{ij}^{\Psi}p^2 + \gamma/\mathrm{th}(l\gamma)\right]/A_{ij}, \quad (24)$$

$$W_{13}(p) = \Xi_1(p)/F_2(p) = W_{22}(p) = \Xi_2(p)/F_1(p) = \left[\chi_{ij}^{\Psi}\gamma/\mathrm{sh}(l\gamma)\right]/A_{ij}, \quad (25)$$

$$W_{23}(p) = \Xi_2(p)/F_2(p) = -\chi_{ij}^{\Psi}\left[M_1\chi_{ij}^{\Psi}p^2 + \gamma/\mathrm{th}(l\gamma)\right]/A_{ij}. \quad (26)$$

Therefore, we obtain from equations (21) the generalized matrix equaion for the electromagnetoelastic actuator

$$\begin{pmatrix}\Xi_1(p)\\ \Xi_2(p)\end{pmatrix} = \begin{pmatrix}W_{11}(p) & W_{12}(p) & W_{13}(p)\\ W_{21}(p) & W_{22}(p) & W_{23}(p)\end{pmatrix}\begin{pmatrix}\Psi_m(p)\\ F_1(p)\\ F_2(p)\end{pmatrix}. \quad (27)$$

Let us find the displacement of the faces the electromagnetoelastic actuator in a stationary regime for $\Psi_m(t) = \Psi_{m0}\cdot 1(t)$, $F_1(t) = F_2(t) = 0$ and inertial load. The static displacement of the faces the electromagnetoelastic actuator $\xi_1(\infty)$ and $\xi_2(\infty)$ can be written in the form

$$\xi_1(\infty) = \lim_{t\to\infty}\xi_1(t) = \lim_{\substack{p\to 0\\ \alpha\to 0}} pW_{11}(p)\Psi_{m0}/p = \nu_{mi}l\Psi_{m0}(M_2 + m/2)/(M_1 + M_2 + m), \quad (28)$$

$$\xi_2(\infty) = \lim_{t\to\infty}\xi_2(t) = \lim_{\substack{p\to 0\\ \alpha\to 0}} pW_{21}(p)\Psi_{m0}/p = \nu_{mi}l\Psi_{m0}(M_1 + m/2)/(M_1 + M_2 + m), \quad (29)$$

$$\xi_1(\infty) + \xi_2(\infty) = \lim_{t\to\infty}(\xi_1(t) + \xi_2(t)) = \nu_{mi}l\Psi_{m0}, \quad (30)$$

where m is the mass of the electromagnetoelastic actuator, M_1, M_2 are the load masses.

Consider a numerical example of the calculation of static characteristics of the piezoactuator from piezoceramics PZT at $m << M_1$ and $m << M_2$. For $d_{33} = 4\cdot 10^{-10}$ m/V, $U = 125$ V, $M_1 = 10$ kg and $M_2 = 40$ kg we obtain the static displacement of the faces of the piezoactuator $\xi_1(\infty) = 40$ nm, $\xi_2(\infty) = 10$ nm, $\xi_1(\infty) + \xi_2(\infty) = 50$ nm.

The static displacement the faces of the piezoactuator for the transverse piezoelectric effect and inertial load at $U(t) = U_0\cdot 1(t)$, $E_3(t) = E_{30}\cdot 1(t) = (U_0/\delta)\cdot 1(t)$ and $F_1(t) = F_2(t) = 0$ can be written in the following form:

$$\xi_1(\infty) = d_{31}(h/\delta)U_0(M_2 + m/2)/(M_1 + M_2 + m), \quad (31)$$

$$\xi_2(\infty) = d_{31}(h/\delta)U_0(M_1 + m/2)/(M_1 + M_2 + m), \quad (32)$$

$$\xi_1(\infty) + \xi_2(\infty) = d_{31}(h/\delta)U_0. \quad (33)$$

Consider a numerical example for the calculation of static characteristics of the piezoactuator from PZT under the transverse piezoeffect at $m << M_1$ and $m << M_2$. For $d_{31} = 2.5\cdot 10^{-10}$ m/V, $h = 4\cdot 10^{-2}$ m, $\delta = 2\cdot 10^{-3}$ m, $U = 250$ V, $M_1 = 10$ kg and $M_2 = 40$ kg we obtain the static displacement of the faces of the piezoactuator $\xi_1(\infty) = 1$ μm, $\xi_2(\infty) = 0.25$ μm, $\xi_1(\infty) + \xi_2(\infty) = 1.25$ μm. The experimental and calculated values for the actuator are in agreement to an accuracy of 5%.

For the description of the piezoactuator for the longitudinal piezoelectric effect for one rigidly fixed face of the transducer at $M_1 \to \infty$ we obtain from equation (23)and (26) the transfer functions $W_{21}(p)$ and $W_{23}(p)$ of the piezoactuator for the longitudinal piezoelectric effect in the following form

$$W_{21}(p) = \Xi_2(p)/E_3(p) = d_{33}\delta/\left[M_2\delta\chi_{33}^{E}p^2 + \delta\gamma\,\mathrm{cth}(\delta\gamma)\right], \quad (34)$$

$$W_{23}(p) = \Xi_2(p)/F_2(p) = -\delta\chi_{33}^{E}/\left[M_2\delta\chi_{33}^{E}p^2 + \delta\gamma\,\mathrm{cth}(\delta\gamma)\right]. \quad (35)$$

Accordingly, the static displacement $\xi_2(\infty)$ of the piezoactuator under the longitudinal piezoeffect in the form

$$\xi_2(\infty) = \lim_{t\to\infty} \xi_2(t) = \lim_{p\to 0} pW_2(p)U_0/p = d_{33}U_0, \quad (36)$$

$$\xi_2(\infty) = \lim_{p\to 0} pW_{23}(p)F_0/p = -\delta s_{33}^E F_0/S_0. \quad (37)$$

Consider a numerical example for the calculation of static characteristics of the piezoactuator for longitudinal piezoeffects. For $d_{33} = 5\cdot 10^{-10}$ m/V, $U = 100$ V we obtain $\xi_2(\infty) = 50$ nm. For $\delta = 6\cdot 10^{-4}$ m, $s_{33}^E = 3.5\cdot 10^{-11}$ m^2/N, $F_0 = 400$ N, $S_0 = 1.75\cdot 10^{-4}$ m^2 we obtain $\xi_2(\infty) = -48$ nm.

Let us consider the operation at low frequencies for the piezoactuator with one face rigidly fixed so that $M_1 \to \infty$ and $m << M_2$. Using the approximation of the hyperbolic cotangent by two terms of the power series in transfer functions (34) and (35), at $m << M_2$ we obtain the expressions in the frequency range of $0 < \omega < 0,01c^E/\delta$

$$W_{21}(p) = \Xi_2(p)/E_3(p) = d_{33}\delta/\left(T_t^2 p^2 + 2T_t\xi_t p + 1\right), \quad (38)$$

$$\begin{aligned} W_{23}(p) &= \Xi_2(p)/F_2(p) \\ &= -\left(s_{33}^E\delta/S_0\right)/\left(T_t^2 p^2 + 2T_t\xi_t p + 1\right), \end{aligned} \quad (39)$$

$$T_t = \left(\delta/c^E\right)\sqrt{M_2/m} = \sqrt{M_2/C_{33}^E},$$

$$\xi_t = (\alpha\delta/3)\sqrt{m/M_2}, C_{33}^E = S_0/\left(s_{33}^E\delta\right) = 1/\left(\chi_{33}^E\delta\right),$$

where T_t is the time constant and ξ_t is the damping coefficient, C_{33}^E - is the is rigidity of the piezoelectric actuator for $E = \text{const}$ under the longitudinal piezoelectric effect.

In the static mode of operation the piezoelectric actuator for elastic load we obtain the equation for its displacement in the following form

$$\xi_2 = \frac{\xi_{2m}}{1 + C_e/C_{33}^E}, \quad (40)$$

where ξ_2 is the displacement of the piezoactuator in the case of the elastic load, $\xi_{2m} = d_{33}U_0$ is the maximum displacement of the piezoactuator, C_e is the load rigidity.

From (38), (40) we obtain the transfer functions of the piezoactuator with a fixed end and elastic inertial load

$$W_2(p) = \frac{\Xi_2(p)}{U(p)} = \frac{d_{33}}{\left(1 + C_e/C_{33}^E\right)\left(T_t^2 p^2 + 2T_t\xi_t p + 1\right)}, \quad (41)$$

where the time constant T_t and the damping coefficient ξ_t are determined by the formulas

$$T_t = \sqrt{M_2/\left(C_e + C_{33}^E\right)},$$

$$\xi_t = \alpha\delta^2 C_{33}^E/\left(3c^E\sqrt{M\left(C_e + C_{33}^E\right)}\right).$$

At low frequencies the experimental and calculated the time constants for the piezoactuators are in agreement to an accuracy of 5%, for example, for the piezoactuator with one face rigidly fixed and elastic inertial load so that $M_1 \to \infty$ and $m << M_2$ for $M_2 = 10$ kg, $C_{33} = 9\cdot 10^6$ N/m, $C_e = 1\cdot 10^6$ N/m we obtain $T_t = 1\cdot 10^{-3}$ c.

4. Results and Discussions

For mechatronics the structural-parametric model and the generalized linear parametric structural schematic diagram of the simple electromagnetoelastic actuator of the mechatronics systems are obtained taking into account equation of generalized electromagnetoelasticity (piezoelectric, piezomagnetic, electrostriction, and magnetostriction effects) and decision wave equation.

The results of constructing the generalized structural-parametric model and the generalized parametric structural schematic diagram of actuator for the longitudinal, transverse and shift deformations are shown in Figure 7.

The parametric structural schematic diagrams piezoelectric actuator for longitudinal, transverse, shift piezoelectric effects Figure 2, Figure 4, Figure 6 converts to the generalized parametric structural schematic diagram of the actuator for the mechatronics systems Figure 7 with the replacement of the following parameters:

$$\Psi_m = E_3, E_3, E_1, \nu_{mi} = d_{33}, d_{31}, d_{15},$$
$$s_{ij}^{\Psi} = s_{33}^E, s_{11}^E, s_{55}^E, l = \delta, h, b.$$

For the mechatronics systems it is possible to construct the generalized structural-parametric model, the generalized parametric structural schematic diagram and the transfer functions in matrix form of the electromagnetoelastic actuator, using the solutions of the wave equation of the actuator and taking into account the features of the deformations actuator along the coordinate axes.

The generalized linear structural-parametric model and the generalized parametric structural schematic diagram of the electromagnetoelastic actuator after algebraic transformations are produced the transfer functions of the electromagnetoelastic actuator for the mechatronics systems.

The piezoelectric actuator with the transverse piezoelectric effect compared to the piezoelectric actuator for the longitudinal piezoelectric effect provides a greater range of static displacement and a less working force and the magnetostriction actuators provides a greater range of static working forces for the mechatronics systems.

5. Conclusions

The parametric structural schematic diagrams and the transfer functions of the piezoactuators for the transverse, longitudinal, shift piezoelectric effects are obtained from linear structural-parametric models of the piezoactuators for the mechatronics systems.

The systems of equations are determined for the linear structural-parametric models of the piezoactuators for mechatronics. Using the obtained solutions of the wave equation and taking into account the features of the

deformations along the coordinate axes, it is possible to construct the generalized linear structural-parametric model and parametric structural schematic diagram of the electromagnetoelastic actuator for the mechatronics systems and to describe its dynamic and static properties.

The transfer functions in matrix form are described the deformations of the electromagnetoelastic actuator during its operation as a part of the mechatronics systems.

References

[1] Przybylski J. "Static and dynamic analysis of a flextensional transducer with an axial piezoelectric actuation," *Engineering structures*, 2015, 84, 140-151.

[2] Afonin, S.M. "Solution of the wave equation for the control of an elecromagnetoelastic transduser," *Doklady mathematics*, 73, 2, 307-313, 2006.

[3] Afonin, S.M. "Structural parametric model of a piezoelectric nanodisplacement transduser," *Doklady physics*, 53, 3, 137-143, 2008.

[4] Ueda J., Secord T., Asada H. H. "Large effective-strain piezoelectric actuators using nested cellular architecture with exponential strain amplification mechanisms," *IEEE/ASME Transactions on Mechatronics*, 2010, 15, 5, 770-782.

[5] Karpelson, M., Wei, G.-Y., Wood, R.J. "Driving high voltage piezoelectric actuators in microrobotic applications," *Sensors and Actuators A: Physical*, 2012, 176, 78-89.

[6] Schultz J., Ueda J., Asada H. *Cellular Actuators*. Oxford: Butterworth-Heinemann Publisher, 2017. 382 p.

[7] Uchino, K. *Piezoelectric actuator and ultrasonic motors*. Boston, MA: Kluwer Academic Publisher, 1997, 347 p.

[8] Gu G.-Y., Yang M.-J., Zhu L.-M. "Real-time inverse hysteresis compensation of piezoelectric actuators with a modified Prandtl-Ishlinskii model," *Review of scientific instruments*, 2012, 83, 6, 065106.

[9] Talakokula V., Bhalla S., Ball R.J., Bowen C.R., Pesce G.L., Kurchania R.,. Bhattacharjee B, Gupta A., Paine K. "Diagnosis of carbonation induced corrosion initiation and progressionin reinforced concrete structures using piezo-impedance transducers," *Sensors and Actuators A: Physical*, 2016, 242, 79-91.

[10] Yang, Y. , Tang, L. "Equivalent circuit modeling of piezoelectric energy harvesters," *Journal of intelligent material systems and structures*, 20, 18, 2223-2235, 2009.

[11] Cady, W.G. *Piezoelectricity an introduction to the theory and applications of electromechancial phenomena in crystals*. New York, London: McGraw-Hill Book Company, 1946, 806 p.

[12] *Physical Acoustics: Principles and Methods*. () Vol.1. Part A. Methods and Devices. Ed.: W. Mason. New York: Academic Press, 1964, 515 p.

[13] Zwillinger, D. *Handbook of Differential Equations*. Boston: Academic Press, 1989, 673 p.

[14] Afonin, S.M. "Structural-parametric model and transfer functions of electroelastic actuator for nano- and microdisplacement, Chapter 9 in *Piezoelectrics and Nanomaterials: Fundamentals, Developments and Applications*. Ed. I.A. Parinov. New York: Nova Science, 2015, pp. 225-242.

[15] Afonin, S.M. "Generalized parametric structural model of a compound elecromagnetoelastic transduser," *Doklady physics*, 50, 2, 77-82, 2005.

[16] Afonin, S.M. "Parametric structural diagram of a piezoelectric converter. *Mechanics of solids*, 37, 6, 85-91, 2002.

[17] Afonin, S.M. "Parametric block diagram and transfer functions of a composite piezoelectric transducer," *Mechanics of solids*, 39, 4, 119-127, 2004.

[18] Afonin, S.M. "Static and dynamic characteristics of a multy-layer electroelastic solid," *Mechanics of solids*, 44, 6, 935-950, 2009.

[19] Afonin, S.M. "Design static and dynamic characteristics of a piezoelectric nanomicrotransducers," *Mechanics of solids*, 45, 1, 123-132, 2010.

[20] Afonin, S.M. "Electroelasticity problems for multilayer nano- and micromotors," *Russian engineering research*, 31, 9, 842-847, 2011.

[21] Afonin, S.M. "Absolute stability conditions for a system controlling the deformation of an elecromagnetoelastic transduser," *Doklady mathematics*, 74, 3, 943-948, 2006.

[22] Afonin, S.M. "Generalized structural-parametric model of an elecromagnetoelastic converter for nano- and micrometric movement control systems: III. Transformation parametric structural circuits of an elecromagnetoelastic converter for nano- and micromovement control systems," *Journal of computer and systems sciences international*, 45, 2, 317-325, 2006.

[23] Afonin, S.M. "Block diagrams of a multilayer piezoelectric motor for nano- and microdisplacements based on the transverse piezoeffect," *Journal of computer and systems sciences international*, 54, 3, 424-439, 2015.

[24] *Springer Handbook of Nanotechnology*. Ed. by B. Bhushan. Berlin, New York: Springer, 2004, 1222 p.

[25] Encyclopedia of Nanoscience and Nanotechnology. Ed. by H. S. Nalwa. Calif.: American Scientific Publishers. 10 Volumes, 2004.